Int. J. Solids Structures Vol. 19, No. 9, pp. 825–837, 1983
Printed in Great Britain.

0020-7683/83 $3.00 + .00
Pergamon Press Ltd

A SINGULAR HYBRID FINITE ELEMENT ANALYSIS OF BOUNDARY-LAYER STRESSES IN COMPOSITE LAMINATES

S. S. WANG and F. G. YUAN
Department of Theoretical and Applied Mechanics, University of Illinois, Urbana, IL 61801, U.S.A.

(*Received* 21 *October* 1981; *in revised form* 3 *May* 1982)

Abstract—A singular hybrid finite element method for studying boundary-layer stresses in composite laminates is presented. The laminate elasticity basis and the fundamental solution structure for the boundary-layer field are briefly reviewed first. Formulation of a singular composite-edge element is based on the recently developed boundary-layer theory and the variational principle of a modified hybrid functional. The singular hybrid element is used conveniently in conjunction with displacement-based conventional elements. Numerical solutions for the well-known Pipes–Pagano problem are presented for illustration. Comparisons of the present solution with the laminate elasticity solution and conventional finite element results are made to demonstrate the accuracy and efficiency of the present approach. Influences of eigenfunction truncation, size and aspect ratio of the singular hybrid element as well as mesh configuration are studied.

1. INTRODUCTION

The presence of geometric boundaries has been well-known to introduce peculiar effects, i.e. the so-called free-edge or boundary-layer effects, in a finite-dimensional composite laminate[1–5]. A very complex state of stress with high gradients has been noted in the vicinity of the edge due to the presence of interlaminar stress to keep the laminae in a state of equilibrium and kinematic compatibility. Interlaminar and intralaminar fracture have been observed to initiate frequently at the edges[6–10]. Laminate static strength and long-term structural load-carrying capacity, especially under fatigue loading, have been closely related to the near-field behavior at laminate boundaries[7, 8, 11–13]. Thus an accurate solution for the boundary-layer stress field is of critical importance in advancing our understanding of the complex fracture behavior and in assisting the design and analyses against failure of composite materials and structures.

Various approximate theories have been proposed in attempts to obtain analytical solutions for the edge stress problem, for example, the higher-order plate theory by Pagano[14], the perturbation approach by Hsu and Herakovich[15], the boundary-layer matching method by Tang and Levy[16], and the recent development based on Reissner's variational principle by Pagano[17]. Numerical approaches such as finite element methods have also been attempted[19–23] due to their versatility in handling complex problems in solid mechanics. Results for the boundary-layer problem obtained from different numerical approaches have shown some similarities. But discrepancies exist in the magnitude and even in the sign of computed stresses in the boundary-layer region. With each refined formulation in the analyses, the maximum value of stress at the laminate edge is shown to rise. Also, the edge stresses are observed to increase as the element size progressively decreases. These discrepancies may result in part from various approximations made in formulation of different analytical and finite element models. But, in the authors' opinion, the fundamental source of the disagreement may be attributed to the singular nature of the boundary-layer stress field, which all of the aforementioned approaches fail to account for. The quests, apparently, are to determine the order of the stress singularity and to establish a complete solution for the problem by an appropriate method. Recently, the exact order of the boundary-layer stress singularity has been obtained for anisotropic composite laminates by using the theory of anisotropic elasticity and an eigenfunction expansion method[24].

In this paper, a new method of finite element analysis for solving the boundary-layer problem is developed based on the recently obtained laminate elasticity solution[24] and the modified hybrid variational functional in [25, 26]. A singular hybrid composite-edge element is constructed by using the eigenfunction series (including both the dominant singular and higher-order terms) determined from the laminate elasticity solution in Ref. [24]. The advanced hybrid, singular element used in

conjunction with conventional isoparametric, quasi three-dimensional elements will be shown to be especially suitable for examining the exact and detailed nature of the boundary-layer stress in composite laminates with general lamination and geometric variables. The method of analysis, as will be demonstrated later, provides extremely efficient computation and accurate solutions for the composite boundary-layer problem.

2. LAMINATE ELASTICITY SOLUTION STRUCTURE FOR STRESS AND DISPLACEMENT FIELDS

A laminate elasticity theory for boundary-layer stress singularities and complete stress solutions has been given in Ref. [24] for finite-dimensional composite laminates. For the convenience of later developments in this paper, some of the fundamental relationships in the laminate elasticity solution are briefly introduced here; detailed derivation can be found in [24] and is, therefore, omitted.

Consider a finite-width composite subjected to surface tractions acting in planes normal to the generator of the lateral surface, i.e. the z-axis, without variation. The special case of a composite laminate subjected to a uniform axial strain, $\epsilon_z = \epsilon_o$, along the z-axis (Fig. 1) has received much attention recently in the investigation of boundary-layer effects in composite laminates. The composite is assumed to be sufficiently long that, in the region away from the ends, end effects are negligible by virtue of Saint Venant's principle. Consequently, stresses in the laminate are independent of the z-axis. This class of problems may be formulated on the basis of theory of anisotropic elasticity by introducing Lekhnitskii's stress potentials, $F(x, y)$ and $\Psi(x, y)$, as

$$\sigma_x = \frac{\partial^2 F}{\partial y^2}, \qquad \sigma_y = \frac{\partial^2 F}{\partial x^2}, \qquad \tau_{xy} = -\frac{\partial^2 F}{\partial x\, \partial y},$$
$$\tau_{xz} = \frac{\partial \Psi}{\partial y}, \qquad \tau_{yz} = -\frac{\partial \Psi}{\partial x}. \tag{1}$$

Following the procedure given in Refs. [24, 27], a system of coupled governing partial differential equations for a composite lamina may be obtained as

$$\begin{cases} L_3 F + L_2 \Psi = -2A_4 + A_1 S_{34} - A_2 S_{35}, \\ L_4 F + L_3 \Psi = 0, \end{cases} \tag{2}$$

where L_2, L_3 and L_4 are linear differential operators of the second, third and fourth orders. A_1, A_2, A_4 are constants related to laminate deformation, and S_{ij} is the lamina compliance tensor. Detailed forms of L_i $(i = 2, 3, 4)$ and A_j $(j = 1, 2, 3, 4)$ are given in [24, 27].

Introducing the complex variables $Z_k = x + \mu_k y$ and choosing the following expression for the stress functions [27], $F = \Sigma_{k=1}^{6} F_k(Z_k)$ and $\Psi = \Sigma_{k=1}^{6} \eta_k F_k'(Z_k)$:

$$F_k(Z_k) = C_k Z_k^{\delta+2}/[(\delta+1)(\delta+2)], \tag{3}$$

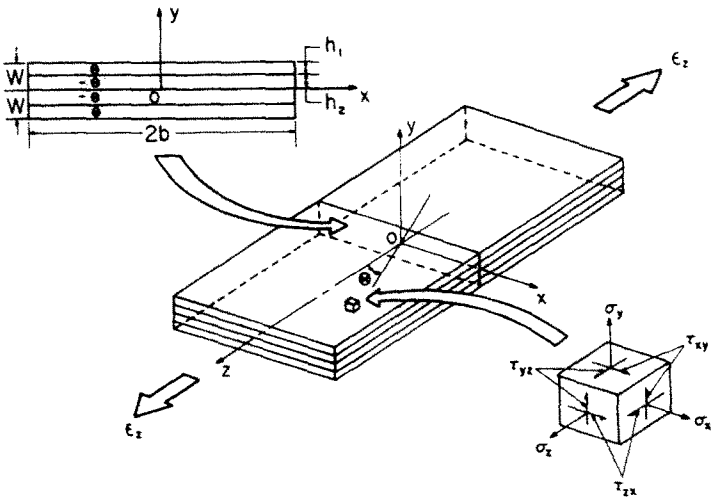

Fig. 1. Geometry of a symmetric $[\theta/-\theta/-\theta/\theta]$ composite laminate subjected to uniform axial extension.

where C_k and δ are complex constants to be determined, one can easily show[24] that general solutions for the stress and displacement have the following forms:

$$\sigma_i = \sum_{n=1}^{\infty} c_{1n}\,\mathrm{Re}\left\{\sum_{k=1}^{3}\left[b_{nk}\Lambda_{ik}Z_k^{\delta_n} + b_{n(k+3)}\bar{\Lambda}_{ik}\bar{Z}_k^{\delta_n}\right]\right\} + \sum_{n=1}^{\infty} c_{2n}\,\mathrm{Im}\left\{\sum_{k=1}^{3}\left[b_{nk}\Lambda_{ik}Z_k^{\delta_n} + b_{n(k+3)}\bar{\Lambda}_{ik}\bar{Z}_k^{\delta_n}\right]\right\} + \sigma_{oi}, \tag{4a}$$

$$u_j = \sum_{n=1}^{\infty} c_{1n}\,\mathrm{Re}\left\{\sum_{k=1}^{3}\left[b_{nk}\Gamma_{(j+3)k}Z_k^{(\delta_n+1)} + b_{n(k+3)}\bar{\Gamma}_{(j+3)k}\bar{Z}_k^{(\delta_n+1)}\right]\Big/(\delta_n+1)\right\} + \sum_{n=1}^{\infty} c_{2n}\,\mathrm{Im}\left\{\sum_{k=1}^{3}\left[b_{nk}\Gamma_{(j+3)k}Z_k^{(\delta_n+1)} + b_{n(k+3)}\bar{\Gamma}_{(j+3)k}\bar{Z}_k^{(\delta_n+1)}\right]\Big/(\delta_n+1)\right\} + u_{oj}, \tag{4b}$$

if δ_n are complex conjugate pairs; and

$$\sigma_i = \sum_{n=1}^{\infty} c_{1n}\left\{\sum_{k=1}^{3}\left[\mathrm{Re}(b_{nk}\Lambda_{ik}Z_k^{\delta_n}) + \mathrm{Im}(b_{n(k+3)}\Lambda_{i(k+3)}\bar{Z}_k^{\delta_n})\right]\right\} + \sigma_{oi}, \tag{5a}$$

$$u_j = \sum_{n=1}^{\infty} c_{1n}\left\{\sum_{k=1}^{3}\left[\mathrm{Re}(b_{nk}\Gamma_{jk}Z_k^{(\delta_n+1)}) + \mathrm{Im}(b_{n(k+3)}\Gamma_{j(k+3)}\bar{Z}_k^{(\delta_n+1)})\right]\Big/(\delta_n+1)\right\} + u_{oj}, \quad (i=1,2,4,5,6;\ j=1,2,3), \tag{5b}$$

if δ_n are distinct and real, where Λ_{ik} and Γ_{jk} are constants related to lamina elastic constants; b_{nk} are known constants related to the eigenvectors, and c_{1n} and c_{2n} are unknown real constants corresponding to the eigenvalue δ_n. Appropriate methods such as the hybrid finite element technique, which will be discussed in the next section, may be used to determine these constants. The σ_{oi} and u_{oj} are particular solutions for stress and displacement in a composite laminate subjected to a given loading condition.

The eigenvalues δ_n, which are determined by using near-field traction boundary conditions on free-edge surfaces and continuity conditions along the ply interface[24], provide important information on the fundamental structure of boundary-layer field solutions. Due to positive definiteness of strain energy of the elastic body, the eigenvalues δ_n bounded by

$$-1 < \mathrm{Re}[\delta_n] < 0 \tag{6}$$

characterize the order of the boundary-layer stress singularity.

3. FINITE ELEMENT FORMULATION

For elasticity problems with stress singularities, it is well-known that using higher-order, conventional (nonsingular) elements may not improve the rate of solution convergence [28]; hence, a very fine mesh with a large number of degrees of freedom (DOF) is generally required. Among various methods proposed for this class of problems, the recently developed hybrid finite elements which incorporate analytical solutions in element formulation have been demonstrated to be most successful. In this section, a hybrid composite-edge element is constructed for the boundary-layer problem, based on the eigenfunction solution determined in Section 2 and the hybrid finite element concept introduced in [25, 26].

3.1 *Stiffness matrix formulation for singular hybrid boundary-layer (edge) element*

To illustrate the basic scheme of stiffness matrix formulation for the composite boundary-layer element, the well-known Pipes–Pagano problem[2] is considered here (Fig. 1) for simplicity and without loss of generality. The element stiffness matrix is formulated on the basis of a modified hybrid variational functional $\pi_{mh}(\boldsymbol{\sigma}, \mathbf{u}, \bar{\mathbf{u}})$ given in [25, 26].

For the present problem, the hybrid functional π_{mh} can be shown[29] to have a slightly

modified form as

$$\pi_{mh}(\bar{\sigma}, \mathbf{u}, \tilde{\mathbf{u}}) = \iint_{A_m} \left(\bar{\sigma}^T \bar{\epsilon} - \frac{1}{2}\bar{\sigma}^T \bar{\mathbf{S}} \bar{\sigma}\right) dA - \int_{\partial A_m} \mathbf{T}^T (\mathbf{u} - \tilde{\mathbf{u}})\, ds - \int_{s_{\sigma_m}} \mathbf{T}^{*T} \tilde{\mathbf{u}}\, ds - \iint_{A_m} \bar{\sigma}^T \bar{\epsilon}_o\, dA + C_o \tag{7}$$

where A_m is the area of the mth element; ∂A_m is the boundary of A_m; s_{σ_m} is the portion of element boundary ∂A_m, where traction $\mathbf{T}^*$ is prescribed; $\tilde{\mathbf{u}}$ is the displacement vector defined over the element boundary, and

$$\bar{\sigma}^T = \{\sigma_x, \sigma_y, \tau_{yz}, \tau_{zx}, \tau_{xy}\}, \qquad \bar{\epsilon}^T = \{\epsilon_x, \epsilon_y, \gamma_{yz}, \gamma_{zx}, \gamma_{xy}\}, \tag{8a}$$

$$\bar{\epsilon}_o{}^T = \{\epsilon_{oi}\} = \{\epsilon_{ox}, \epsilon_{oy}, \gamma_{oyz}, \gamma_{ozx}, \gamma_{oxy}\}, \qquad \mathbf{u}^T = \{u, v, w\}, \tag{8b}$$

with

$$\epsilon_{oi} = \frac{S_{i3}}{S_{33}} \epsilon_0, \qquad C_o = \frac{1}{2} \iint_{A_m} \frac{\epsilon_o^2}{S_{33}} dA, \tag{8c}$$

and $\bar{\mathbf{S}} = \{\bar{S}_{ij}\}$ is the reduced compliance matrix defined in [24]. Note that standard matrix notations, $\bar{\mathbf{S}}$, $\bar{\sigma}$, $\bar{\epsilon}$, $\mathbf{u}$ and $\mathbf{T}$, are used here to represent the compliance matrix, stress, strain, and displacement in the element, and traction along the element boundary, respectively.

The hybrid finite element approach requires that the stress and displacement, $\bar{\sigma}$ and $\mathbf{u}$, within the element and the boundary displacement, $\tilde{\mathbf{u}}$, be independently assumed. Since the general structure of solutions for the laminate elasticity problem has been determined explicitly in the previous section, the stress and displacement expressions given by eqns (4) and (5) can be used directly for the hybrid element stiffness matrix formulation. Thus, the relationships for $\bar{\sigma}$ and $\mathbf{u}$ in the singular hybrid element can be immediately established as

$$\sigma_i = \sum_{n=1}^{N_1} \beta_n \left(\sum_{k=1}^{3} \{\mathrm{Re}[f_{ik}^{(n)}(Z_k)] + \mathrm{Im}[f_{i(k+3)}^{(n)}(\bar{Z}_k)]\} \right) + \sigma_{oi}, \tag{9a}$$

$$u_j = \sum_{n=1}^{N_1} \beta_n \left(\sum_{k=1}^{3} \{\mathrm{Re}[g_{jk}^{(n)}(Z_k)] + \mathrm{Im}[g_{j(k+3)}^{(n)}(\bar{Z}_k)]\} \right) + u_{oj}, \tag{9b}$$

if δ_n are real, and N_1 is the number of distinct, nonzero real δ_n selected; and

$$\sigma_i = \sum_{n=N_1+1}^{N-1} \left\{ \beta_n \,\mathrm{Re}\left[\sum_{k=1}^{6} f_{ik}^{(n)}(Z_k) \right] + \beta_{n+1} \,\mathrm{Im}\left[\sum_{k=1}^{6} f_{ik}^{(n)}(Z_k) \right] \right\} + \sigma_{oi}, \tag{10a}$$

$$u_j = \sum_{n=N_1+1}^{N-1} \left\{ \beta_n \,\mathrm{Re}\left[\sum_{k=1}^{6} g_{jk}^{(n)}(Z_k) \right] + \beta_{n+1} \,\mathrm{Im}\left[\sum_{k=1}^{6} g_{jk}^{(n)}(Z_k) \right] \right\} + u_{oj},$$

$$(i = 1, 2, 4, 5, 6;\ j = 1, 2, 3), \tag{10b}$$

if δ_n are complex conjugates, where N denotes the total number of terms in the truncated eigenfunction series; the unknown stress parameters β_i are real constants to be determined in the finite element analysis, and $f_{ik}^{(n)}$ and $g_{jk}^{(n)}$ are known eigenfunctions determined from eqns (4) and (5).

Expressed in matrix notation, the element stresses, boundary tractions and interior displacements take the forms as

$$\bar{\sigma} = \bar{\mathbf{P}}\boldsymbol{\beta} + \bar{\sigma}_o, \qquad \mathbf{T} = \mathbf{R}\boldsymbol{\beta} + \mathbf{T}_o, \qquad \mathbf{u} = \mathbf{U}\boldsymbol{\beta} + \mathbf{u}_o, \tag{11}$$

where $\boldsymbol{\beta}^T = \{\beta_1, \beta_2, \beta_3, \ldots\}$, and $\bar{\sigma}_o$, $\mathbf{T}_o$ and $\mathbf{u}_o$ are known quantities resulting from particular solutions for stress and displacement. The problem of matching the singular hybrid composite-edge element with adjacent nonsingular elements is resolved by expressing the boundary

displacement $\tilde{\mathbf{u}}$ in terms of element nodal displacement $\mathbf{q}$ as

$$\tilde{\mathbf{u}} = \mathbf{L}\mathbf{q}, \tag{12}$$

where $\mathbf{L}$ is a matrix of properly selected shape functions defined along the hybrid element boundary. The $\mathbf{L}$ is chosen such that, when corresponding nodal displacements of an adjacent element are matched, $\tilde{\mathbf{u}}$ is the same for the two elements over the common boundaries.

In the present finite element approach, a nine-node, hybrid composite-edge element shown in Fig. 2 with 27 degrees of freedom (3 DOF per node) is constructed. Standard quadratic interpolation functions are used for the $\mathbf{L}$ to ensure matching the boundary displacements of the singular hybrid element with those of adjacent eight-node (24 DOF), isoparametric regular elements.

Following the similar formulation of derivation for hybrid finite elements [25, 26], the variational functional may now be expressed in terms of $\boldsymbol{\beta}$ and $\mathbf{q}$ as

$$\pi_{mh} = -\frac{1}{2}\boldsymbol{\beta}^T \mathbf{H}\boldsymbol{\beta} + \boldsymbol{\beta}^T \mathbf{G}\mathbf{q} - \boldsymbol{\beta}^T \mathbf{I} + \mathbf{J}\mathbf{q} + C_o^*, \tag{13}$$

where

$$\mathbf{H} = \frac{1}{2}\int_{\partial A_m} (\mathbf{R}^T \mathbf{U} + \mathbf{U}^T \mathbf{R})\, ds, \qquad \mathbf{G} = \int_{\partial A_m} \mathbf{R}^T \mathbf{L}\, ds, \tag{14a}$$

$$\mathbf{I} = \frac{1}{2}\int_{\partial A_m} \mathbf{R}^T \mathbf{u}_o\, ds + \frac{1}{2}\int_{\partial A_m} \mathbf{U}^T \mathbf{T}_o\, ds + \frac{1}{2}\iint_{A_m} \bar{\mathbf{P}}^T \bar{\boldsymbol{\epsilon}}_o\, dA, \tag{14b}$$

$$\mathbf{J} = \int_{\partial A_m} \mathbf{T}_o{}^T \mathbf{L}\, ds, \tag{14c}$$

$$C_o^* = C_o - \frac{1}{2}\int_{\partial A_m} \mathbf{T}_o{}^T \mathbf{u}_o\, ds - \frac{1}{2}\iint_{A_m} \bar{\boldsymbol{\sigma}}_o{}^T \bar{\boldsymbol{\epsilon}}_o\, dA. \tag{14d}$$

Taking variation of π_{mh} with respect to $\boldsymbol{\beta}$ and $\mathbf{q}$, one obtains the stiffness matrix $\mathbf{k}_s$ and the consistent loading vector $\mathbf{Q}_s$ for the hybrid composite-edge element as

$$\mathbf{k}_s = \mathbf{G}^T \mathbf{H}^{-1} \mathbf{G} \tag{15a}$$

$$\mathbf{Q}_s = \mathbf{G}^T \mathbf{H}^{-1} \mathbf{I} - \mathbf{J}^T, \tag{15b}$$

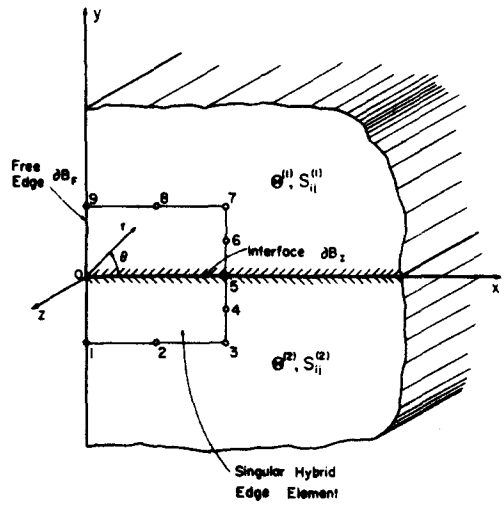

Fig. 2. Coordinates and a singular hybrid boundary-layer element for the composite free-edge problem.

with

$$\boldsymbol{\beta} = \mathbf{H}^{-1}(\mathbf{G}\mathbf{q} - \mathbf{I}). \tag{15c}$$

3.2 *Non-singular element formulation*

The adjacent elements are formulated on the basis of generalized plane deformation theory[27] and the minimum potential energy principle. Because no singularity is involved, formulation of the displacement-based conventional elements is relatively simple. A constant-strain triangular element of the same nature was first proposed by Herakovich *et al.*[19]. To improve the rate of convergence and the accuracy of stress and displacement solutions adjacent to the singular domain, a second-order, eight-node (24 DOF) isoparametric element is developed in this study in conjunction with the construction of the singular hybrid composite-edge element. Derivation of the stiffness matrix $\mathbf{k}_r$ and the loading vector $\mathbf{Q}_r$ for the far-field elements is reported in [29].

3.3 *Solution procedure*

The matrices $\mathbf{k}_s$ and $\boldsymbol{k}_r$ are true stiffness matrices relating unknown nodal displacements to nodal loading vectors. The standard procedure of the matrix-displacement method can be used to assemble the global stiffness matrix and loading vector, $\mathbf{K}$ and $\mathbf{Q}$, leading to the following relationship:

$$\mathbf{K}\mathbf{q} = \mathbf{Q}, \tag{16}$$

where the assemblage process may be expressed symbolically by

$$\mathbf{K} = \sum_m \mathbf{k}_r^{(m)} + \mathbf{k}_s, \tag{17a}$$

$$\mathbf{Q} = \sum_m \mathbf{Q}_r^{(m)} + \mathbf{Q}_s. \tag{17b}$$

After the displacement solution $\mathbf{q}$ is determined, stresses at any point in the singular hybrid element may be calculated by eqn (11), and boundary-layer stress intensity factors, K_i, defined in [24] can be obtained directly from the parameter β_1 of eqn (15c) in the hybrid finite element formulation by

$$K_i = \beta_1 \left\{ \sum_{k=1}^{3} [\mathrm{Re}(b_{1k}\Lambda_{ik}) + \mathrm{Im}(b_{1(k+3)}\Lambda_{i(k+3)})] \right\} \tag{18a}$$

$$K_3 = -S_{3i}K_i/S_{33} \qquad (i = 1, 2, 4, 5, 6), \tag{18b}$$

where the repeated subscript, i, refers to summation of associated quantities.

4. NUMERICAL RESULTS

To demonstrate the effectiveness and the efficiency of the present method of approach, a symmetric angle-ply composite shown in Fig. 1 is considered. Numerical results on solution accuracy, convergence, and several unique features of the method are given for a [45°/−45°/−45°/45°] graphite-epoxy composite for illustration. The composite has a geometry (Fig. 1) of $b/h = 8$ and $h_1 = h_2 = h = 0.25$ in., and elastic ply properties of unidirectional high-modulus graphite-epoxy lamina identical to those in [2, 15, 21] are used. Due to geometric and lamination symmetry, only a quarter of the cross sectional area is considered. Solutions are obtained first by employing eight-node, isoparametric nonsingular elements only. A combination of the singular hybrid element and nonsingular isoparametric elements (Fig. 3) is then used to examine the boundary-layer field in detail. Comparisons of the present solutions with the laminate elasticity solution[24] are made to illustrate the basic nature of computational mechanics for this singular elasticity problem. Influences of eigenfunction truncation in the singular element formulation, geometry of the special hybrid element, and the overall finite-element discretization on the

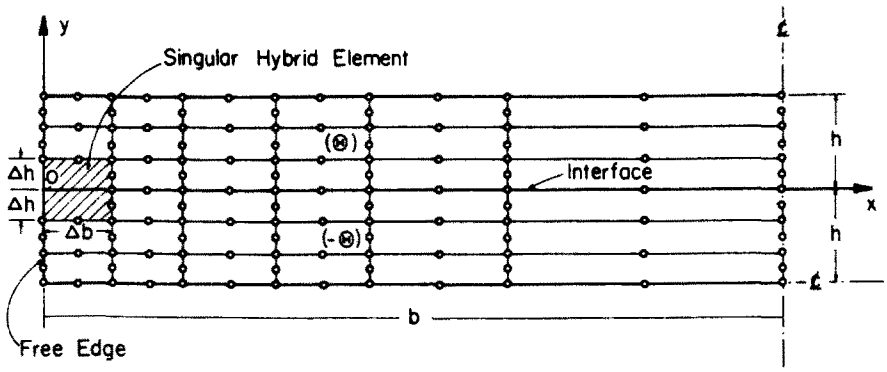

Fig. 3. Singular hybrid element incorporated in a nonsingular isoparametric finite element mesh for the boundary-layer problem in a composite laminate.

accuracy and efficiency of the present approach are discussed. Both the near-field stress (in terms of boundary-layer stress intensity factors) and the overall stress distribution are examined.

In studying the accuracy and convergence of present numerical solutions, the boundary-layer stress intensity factors K_i given in Ref. [24] for the [45°/−45°/−45°/45°] graphite-epoxy composite are used as a reference:

$$K_1^o = 0.57298\ E\ 0, \qquad K_2^o = -0.75345\ E\ 1, \qquad K_3^o = -0.29523\ E{-}1,$$
$$K_4^o = 0.16443\ E\ 2, \qquad K_5^o = 0.14440\ E\ 1, \qquad K_6^o = 0., \tag{19}$$

where K_i^o carry the dimension of [psi-in$^{-\delta_1}$] with $\delta_1 = -0.02558$.

4.1 *Solutions by nonsingular, displacement-based finite elements*

Results from displacement-based finite elements with several different meshes and from Ref. [24] are shown in Fig. 4. (The m in the figure refers to the number of elements per ply through the laminate thickness direction. For example, in the case of $m = 3$, 78 elements with 273 nodes are used.) The in-plane stresses, σ_z and τ_{xz}, determined by the conventional elements decrease as the laminate boundary ($x/b = 1$) is approached. These results are contrary to the laminate elasticity solution [24]. Refining the mesh does not change the nature of the numerical results. The discrepancy between the elasticity solution and the finite element solution increases as the laminate edge is approached, owing to the boundary-layer stress singularity. The present results support the assessment in [28] that conventional finite-element solutions generally converge very slowly for elasticity problems with singularities. The discrepancy clearly indicates the need of an advanced boundary-layer element to include the edge stress singularity for improved solutions.

4.2 *Solutions by singular hybrid finite element method*

A typical mesh consisting of the singular hybrid element and surrounding nonsingular elements is shown in Fig. 3. The singular element contains two dissimilar materials and has a square configuration unless specified otherwise. Numerical solutions obtained for the boundary-layer stress by the singular hybrid FEM are found to differ from the reference elasticity solution [24] within 2% in general. For illustration, stress solutions determined by the singular hybrid element approach with several meshes are shown in Fig. 5. Also shown in the figure are the results from Refs. [21, 24]. All the three different approaches yield the same results in the far field. Near the laminate edge, deviations of σ_z and τ_{xz} from Ref. [24] become significant and an opposite trend of change in stress is observed. It is noted that the results given by [21] were obtained from a mesh having a large number of constant-strain triangular elements (392 elements) with very small size (sixteen elements per ply in the thickness direction). However, with much fewer elements (e.g. 35 elements in the present case) the present singular hybrid element solutions are in excellent agreement with the laminate elasticity solution [24].

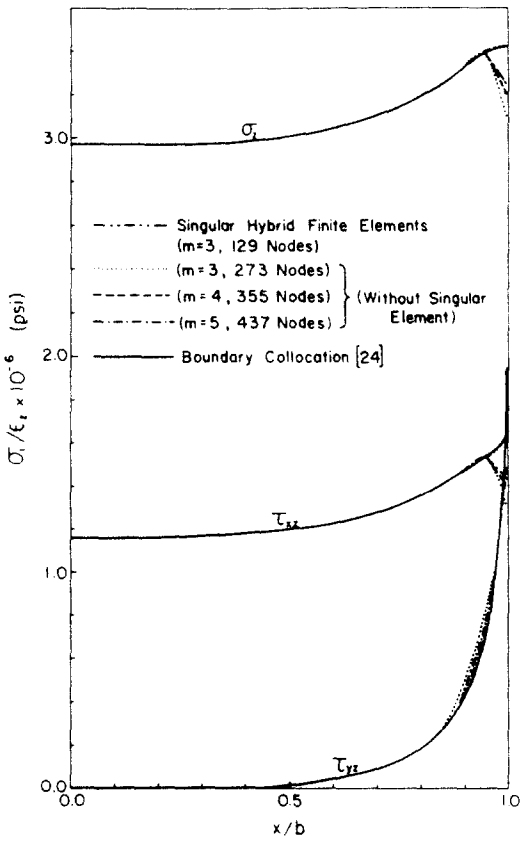

Fig. 4. Comparison of stresses σ_i along the ply interface $y = h$ from Ref. [24] with those from singular hybrid finite-element and conventional finite-element solutions with different meshes.

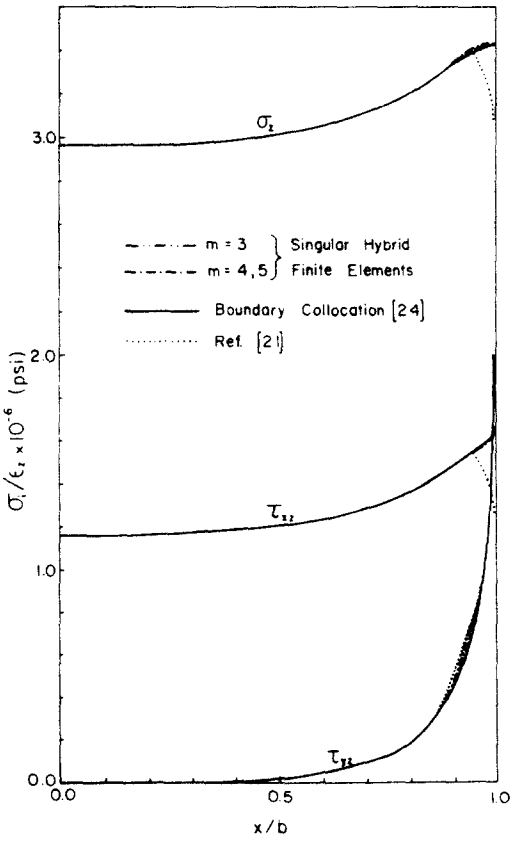

Fig. 5. Comparison of boundary-layer stress solutions σ_z, τ_{xz} and τ_{yz} along the 45°/ − 45° ply interface obtained by various methods of analysis.

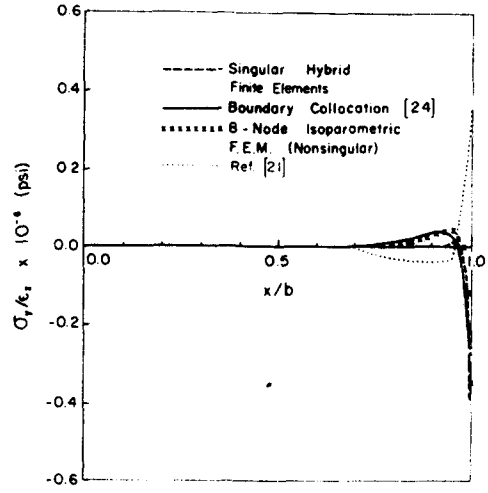

Fig. 6. Comparison of interlaminar normal stress σ_y along the 45°/ − 45° ply interface obtained by various methods of analysis.

Distributions of interlaminar stresses shown in Figs. 5 and 6 reveal some serious problems in the conventional finite element approach. For example, the interlaminar normal stress σ_y near the edge is shown to be highly compressive in the laminate elasticity solution, in the present hybrid element approach, and in the isoparametric finite element analysis. This is apparently opposite to the results of Ref. [21]. The compressive σ_y is consistent with the negative values of the boundary-layer stress intensity factor K_2, i.e.

$$K_2^o = -0.75345 \; E\;1 \quad \text{(from the laminate elasticity solution [24])},$$
$$K_2 = -0.73911 \; E\;1 \quad \text{(from the present singular hybrid FEM)}, \tag{20}$$

determined by the two independent approaches, both including the leading singular and higher order terms in the formulation. Furthermore, K_6 is shown to be zero in both the elasticity solution and the present singular hybrid element solution, which leads to a vanishing τ_{xy} at the laminate boundary, where the conventional finite elements yield a high negative value (Fig. 7).

The discrepancies among these various approaches may result not only from the inclusion of dominant singular terms in the present solution, but also from approximations introduced by lengthy extrapolation required in conventional finite elements for determining stresses along the ply interface and at laminate edges, where stress gradients change most appreciably. This situation

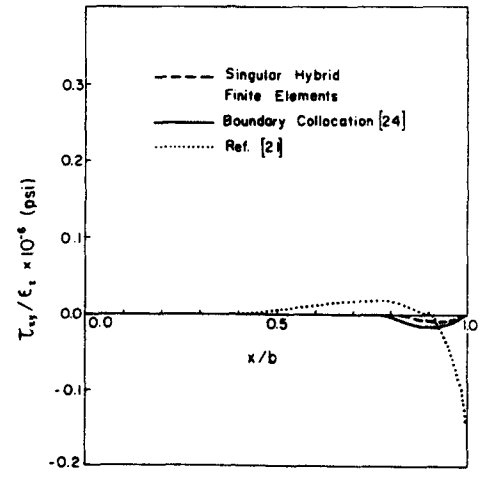

Fig. 7. Comparison of interlaminar shear stress τ_{xy} along the 45°/–45° ply interface obtained by various methods of analysis.

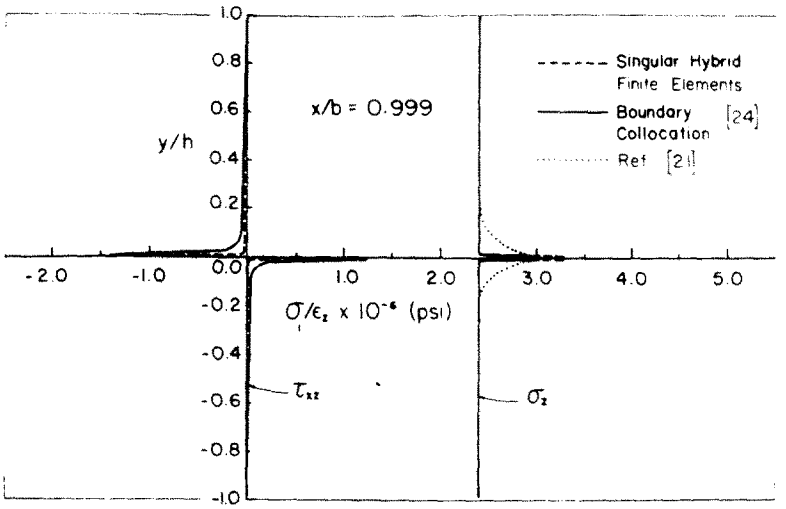

Fig. 8. Through-laminate-thickness distributions of σ_z and τ_{xz} at $x/b = 0.999$ obtained by various methods of analysis.

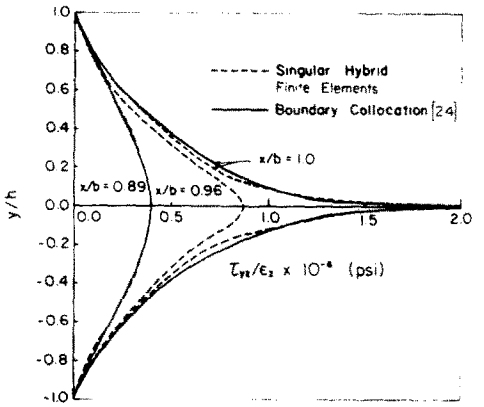

Fig. 9. Through-laminate-thickness distributions of τ_{yz} at $x/b = 1.0$, 0.96 and 0.89, obtained by various methods of analysis.

is illustrated in Figs. 8 and 9, in which boundary-layer stresses in the laminate thickness direction are given. The σ_z and τ_{xz} in Fig. 8, for instance, change very rapidly within an extremely small region near the ply interface, where conventional finite element approaches may fail to approximate. However, the rapid change of stress gradient is clearly observed in the present hybrid FEM results and the laminate elasticity solution[24].

4.3 *Eigenfunction truncation in singular hybrid element formulation*

In the hybrid element formulation, eigenfunction truncation, i.e. the number of terms used in the eigenfunction series, needs to be considered properly. The influence of eigenfunction truncation may be determined by examining the boundary-layer stress intensity solutions. Results are given in Table 1 for the cases of different numbers of eigenfunctions, N, used in analyzing the composite (35 elements and 129 nodes). The effect of eigenfunction truncation on the hybrid element solution for the present problem is very small—generally within a few percent. For example, increasing the number of eigenfunctions from 9 to 23 only alters the results by approximately 1%. Thus, incorporating the first few terms of the eigenfunction series in the special hybrid element ensures the solution accuracy and convergence. Furthermore, the use of only 35 elements (including the singular hybrid one), which gives a solution within 2% of that in Ref. [24], clearly demonstrates the efficiency and the accuracy of the present method of approach.

Table 1. Effect of eigenfunction truncation in singular hybrid element formulation† on free-edge stress intensity factors§

N	K_1	K_2	K_3	K_4	K_5	K_6
9	0.56848	-7.47524	-0.02929	16.31330	1.43265	0.
12	0.56282	-7.40137	-0.02900	16.15210	1.41849	0.
17	0.56249	-7.39644	-0.02898	16.14134	1.41755	0.
20	0.56208	-7.39114	-0.02896	16.12976	1.41653	0.
23	0.56208	-7.39114	-0.02896	16.12977	1.41653	0.

†Square singular element with $\Delta b = 2\Delta h$ and $\eta = 0.4$.

§All K_i are scaled by $10^6 \varepsilon_0$.

4.4 *Size effect of the singular hybrid element*

The special hybrid element is required to cover a finite region of proper size so that the behavior of the singular domain can be fully accounted for. Size effects of the hybrid element on accuracy and convergence of the solution may be characterized by a nondimensional parameter η defined as

$$\eta = \frac{\Delta h}{h} = \frac{\text{linear dimension of the hybrid element}}{\text{laminar thickness}}, \tag{21}$$

where Δh and h are shown in Fig. 3. In the singular hybrid element analysis employing 20 terms in the eigenfunction series, changing the η from 0.24 to 0.5 (i.e. the singular square element with its linear dimension increasing from a quarter to a half lamina thickness) causes less than 1% difference in the edge stress intensity solutions (Table 2). Thus the influence of the singular stress domain is small and fully covered by the singular hybrid element, and stable and converged solutions are obtainable. Also, very large singular elements, say, about a half ply thickness, can be used to determine the edge stress field, thereby, giving efficient computation with much fewer elements. Detailed results on the influence of size of the singular hybrid element on the boundary-layer stress are given in [29].

Table 2. Influence of singular hybrid element size† on boundary-layer stress intensity solutions

η	K_1	K_2	K_3	K_4	K_5	K_6
0.24	0.56226	-7.39349	-0.02897	16.13489	1.41698	0.
0.33	0.56249	-7.39648	-0.02898	16.14143	1.41756	0.
0.4	0.56208	-7.39114	-0.02896	16.12976	1.41653	0.
0.5	0.56477	-7.42649	-0.02910	16.20691	1.42331	0.

†Singular element with $\Delta b = 2\Delta h$ and $\eta = (\Delta h)/h$.

4.5 *Influence of aspect ratio of the singular hybrid element*

Another parameter that may affect the finite element solution is the aspect ratio of the singular hybrid element, defined as

$$\xi = \frac{\Delta b}{2\Delta h}, \tag{22}$$

where Δb and $2\Delta h$ are the width and depth of the element, respectively. Numerical experiments are conducted to identify the influence of ξ on the boundary-layer stress solution. The cases of $\xi = 1.0$, 2.34, 3.75 and 6.25 have been examined, and results are given in Table 3 for illustration. In studying the influence of the hybrid element aspect ratio, the number of nodes and elements are retained the same so as to isolate the effect of changing ξ. The results given in the table indicate that deviations of K_1 from Ref. [24] are again observed within 1% in all cases investigated.

Table 3. Effect of aspect ratio of singular hybrid element† on boundary-layer stress intensity factors*

ξ	K_1	K_2	K_3	K_4	K_5	K_6
1.00	0.56208	-7.39114	-0.02896	16.12976	1.41653	0.
2.34	0.56438	-7.42137	-0.02908	16.19574	1.42232	0.
3.75	0.56484	-7.42738	-0.02910	16.20884	1.42348	0.
6.25	0.56525	-7.43286	-0.02912	16.22081	1.42453	0.

†$\xi = \Delta b/(2\Delta h)$, $(\Delta h)/h = 0.4$, Δb changes with ξ.

*35 elements with 129 nodes and N = 20 are used.

Table 4. Influence of the number of elements through lamina thickness, m, on boundary-layer stress intensity factors*

m	K_1	K_2	K_3	K_4	K_5	K_6
2	0.56207	-7.39095	-0.02896	16.12936	1.41650	0.
3	0.56208	-7.39114	-0.02896	16.12976	1.41653	0.
4	0.56209	-7.39119	-0.02896	16.12987	1.41654	0.
5	0.56209	-7.39120	-0.02896	16.12989	1.41654	0.

*$N = 20$, $\Delta h = 2\Delta h$, $\eta = 0.4$.

4.6 *Effects of the number of elements through lamina thickness*

The rapid change of stress through laminate thickness in the boundary layer generally requires a large number of elements with higher-order interpolation functions and very small element size through the thickness direction in a conventional finite element approach. For example, 16 elements per ply in the laminate-thickness direction were used in Ref. [21]. If, however, functions with the exact order of stress singularities, such as the present eigenfunction series, are included in the hybrid element formulation, fewer elements through ply thickness may be required to provide an accurate description of the stress gradient. Thus, less computing effort is needed and better results should be achieved. This is indeed observed in Table 4 in which the K_i remain almost unchanged when the number of elements per ply increases from 2 to 5. The insensitivity of the K_i to the number of elements through the laminate thickness direction clearly illustrates the efficiency and the accuracy of the present approach. The accuracy and convergence of the stress solutions with different numbers of elements in the lamina thickness direction are also shown in Fig. 5. From the figure and Table 4, it is apparent that with fewer than two or three elements per ply, the solution obtained by the singular hybrid finite element method can be very accurate.

Acknowledgements—The research work described in this paper was supported in part by the Office of Naval Research (ONR), Arlington, Virginia, under grant N000-14-79-C-0579. The authors are grateful to Drs. N. Perrone and Y. Rajapakse of ONR for the encouragement. The authors are also indebted to Prof. H. T. Corten of the University of Illinois and Dr. C. C. Chamis of NASA-Lewis Research Center for the fruitful discussion during the course of this study.

REFERENCES

1. A. H. Puppo and H. A. Evensen, Interlaminar shear in laminated composites under generalized plane stresses. *J. Composite Matls* **4**, 204–220 (1970).
2. R. B. Pipes and N. J. Pagano, Interlaminar stresses in composite laminates under uniform axial extension. *J. Composite Matls* **4**, 538–548 (1970).
3. R. L. Foye and D. J. Baker, Design of orthotropic laminates. Presented in the *11th Ann. AIAA Structures, Structural Dynamics, and Materials Conf.*, Denver, Colorado, April 1970.
4. N. J. Pagano and R. B. Pipes, Influence of stacking sequence on laminate strength. *J. Composite Matls* **5**, 51–57 (1971).
5. R. B. Pipes and I. M. Daniel, Moiré analysis of the interlaminar shear edge effect in laminated composites. *J. Composite Matls* **5**, 255–259 (1971).
6. B. E. Kaminski, On the determination of the failure surface for an orthotropic quasi-homogeneous material. Master's Thesis, Georgia Institute of Technology, June 1969.
7. J. M. Whitney, Free-edge effects in the characterization of composite materials. *Analysis of the Test Methods for High Modulus Fibers and Composites, ASTM STP* 521, pp. 167–180 (1973).
8. R. B. Pipes, B. E. Kaminski and N. J. Pagano, Influence of the free edge upon the strength of angle-ply laminates. *Analysis of the Test Methods for High Modulus Fibers and Composites, ASTM STP* 521, 218–228 (1973).

9. N. J. Pagano and R. B. Pipes, Some observations on the interlaminar strength of composite laminates. *Int. J. Mech. Sci.* **15**, 679–688 (1973).
10. F. H. Chang, D. E. Gordon, B. T. Rodini and R. H. McDaniel, Real-time characterization of damage growth in graphite/epoxy laminates. *J. Composite Matls* **10**, 182–192 (1976).
11. M. E. Waddoups, J. R. Eisenmann and B. E. Kaminski, Macroscopic fracture mechanics of advanced composite materials. *J. Composite Matls* **5**, 446–454 (1971).
12. J. M. Whitney and R. J. Nuismer, Stress fracture criteria for laminated composites containing stress concentrations. *J. Composite Matls* **8**, 253–265 (1974).
13. I. M. Daniel, R. E. Rowlands and J. B. Whiteside, Effects of material and stacking sequence on behavior of composite plates with holes. *Experimental Mech.* **14**, 1–9 (1974).
14. N. J. Pagano, On the calculation of interlaminar normal stress in composite laminates. *J. Composite Matls* **8**, 65–81 (1974).
15. P. W. Hsu and C. T. Herakovich, Edge effects in angle-ply composite laminates. *J. Composite Matls* **11**, 422–428 (1977).
16. S. Tang and A. Levy, A boundary layer theory—II. Extension of laminated finite strip. *J. Composite Matls* **9**, 42–45 (1975).
17. N. J. Pagano, Free-edge stress fields in composite laminates. *Int. J. Solids Structures* **14**, 401–406 (1978).
18. E. F. Rybicki, Approximate three-dimensional solutions for symmetric laminates under inplane loading. *J. Composite Matls* **5**, 354–360 (1971).
19. C. T. Herakovich, G. D. Renieri and H. F. Brinson, Finite element analysis of mechanical and thermal edge effects in composite laminates. 1976 *Army Symp. Solid Mechanics, Composite Materials: The Influence of Mechanics of Failure on Design*, Cape Cod, MA., pp. 237–248, Sept. 1976.
20. C. T. Herakovich, A. Nagarkar and D. A. O'Brien, Failure analysis of composite laminates with free edges. *Modern Developments in Composite Materials and Structures* (Edited by J. R. Vinson), pp. 53–56. ASME, New York (1979).
21. A. S. D. Wang and F. W. Crossman, Some new results on edge effect in symmetric composite laminates. *J. Composite Matls* **11**, 92–106 (1977).
22. R. L. Spilker and S. C. Chou, Edge effects in symmetric composite laminates. *J. Composite Matls* **14**, 2-20 (1980).
23. R. L. Spilker, A hybrid-stress finite element formulation for thick multilayer laminates. *Comput. Structures* **11**, 507–514 (1980).
24. S. S. Wang and I. Choi, Boundary-layer effects in composite laminates—I. Free-edge stress singularities—II. Free-edge stress solutions and basic characteristics. *J. Appl. Mech.*, Trans. ASME **49**, 541–560 (1982).
25. P. Tong, T. H. H. Pian and S. J. Lasry, A hybrid-element approach to crack problems in plane elasticity. *Int. J. Num. Meth. Engng* **7**, 297–308 (1973).
26. K. Y. Lin and J. W. Mar, Finite element analysis of stress intensity factors for cracks at a bi-material interface. *Int. J. Fracture* **12**, 521–531 (1976).
27. S. G. Lekhnitskii, *Theory of Elasticity of an Anisotropic Body*. Holden-Day, San Francisco (1963).
28. P. Tong and T. H. H. Pian, On the convergence of the finite element methods for problems with singularity. *Int. J. Solids Structures* **9**, 313–321 (1973).
29. S. S. Wang and F. G. Yuan, A singular hybrid finite element analysis of boundary-layer stresses in composite laminates—I. Theory and formulation—II. Numerical results ONR Contract Reports, Office of Naval Research, Arlington, VA, 1982.